

Sensor and Simulation Notes

Note 95

31 December 1969

A Sloped Admittance Sheet Plus Coplanar Conducting
Flanges as a Matched Termination of a Two-Dimensional
Parallel-Plate Transmission Line

Capt Carl E. Baum
Air Force Weapons Laboratory

Abstract

This note considers the characteristics required of a planar admittance-sheet terminator with coplanar conducting flanges. This admittance sheet terminates an infinitely wide parallel-plate transmission line. The sheet (plus flanges) is sloped at some arbitrary angle with respect to the transmission line. The required surface current density on the admittance sheet is compared to that on a distributed LR termination (using the incident electric field for the calculation); this is used for choosing a good value for the surface inductance. Sloping the termination makes the required current for an ideal termination more quickly approach its late-time (or low-frequency) value which should be a useful feature in realizing good quality distributed terminations.

CLEARED FOR PUBLIC RELEASE

PL-94-1090, 13 Dec 94

I. Introduction

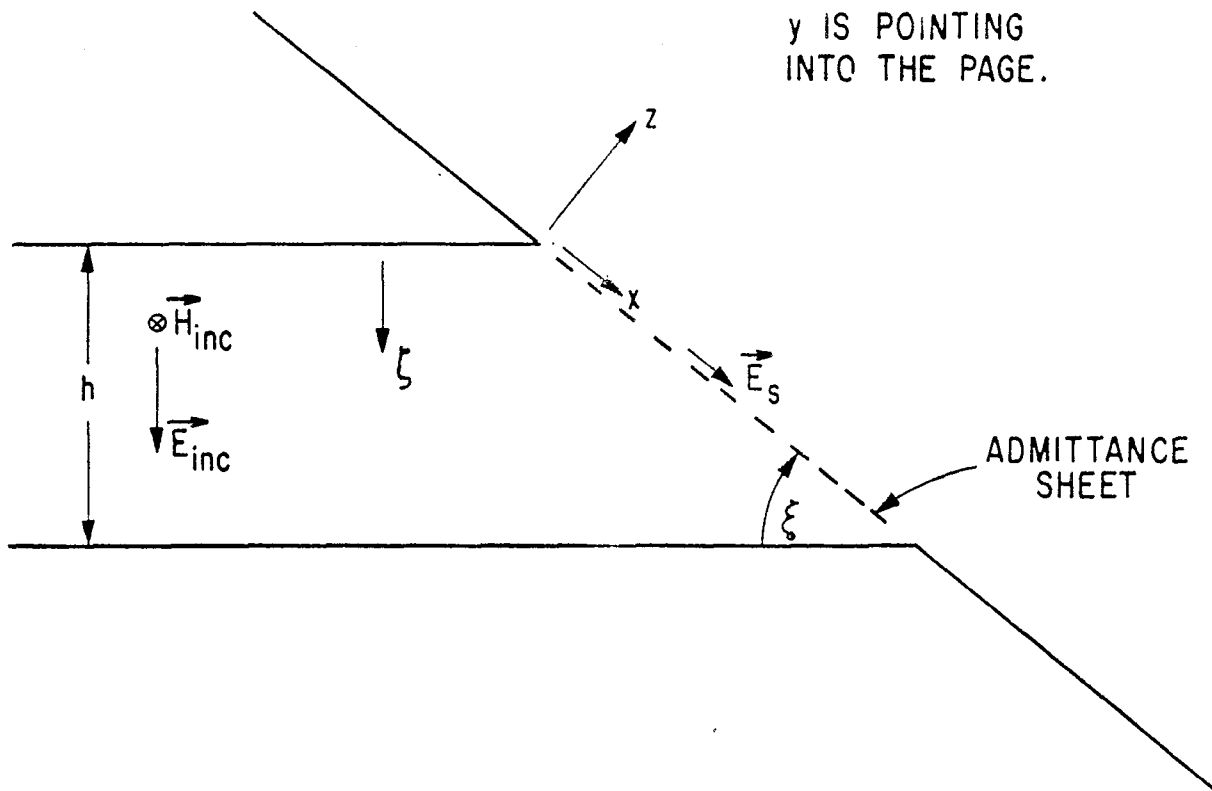
In an earlier note¹ we introduced the concept of an admittance sheet as a distributed termination for a TEM transmission line. In appropriate geometries the required characteristics of such an admittance sheet to provide a perfect termination can be determined from the solution of an electromagnetic boundary value problem. However, the required surface admittance on the sheet may not be completely realizable as passive lumped elements. A first order approximation to the surface admittance uses series inductance and resistance to give what we might call a distributed LR termination. While a distributed LR termination is not in general a perfect termination it can match the ideal admittance in both high and low frequency limits. The surface resistance is chosen to match the low frequency limit of the ideal surface impedance. The surface inductance is chosen to minimize the reflections for frequencies with wavelengths of the order of the cross-section dimensions of the transmission line. A convenient way to choose the inductance is to calculate the ideal surface current density on the ideal termination and compare it to the surface current density associated with a step function electric field on the distributed LR termination.

Another note² has given a detailed calculation of the characteristics of an ideal admittance sheet which terminates two parallel plates and is perpendicular to the direction of incidence of the TEM wave between the plates. Values for the surface inductance in an LR termination to approximate the ideal termination are also given.

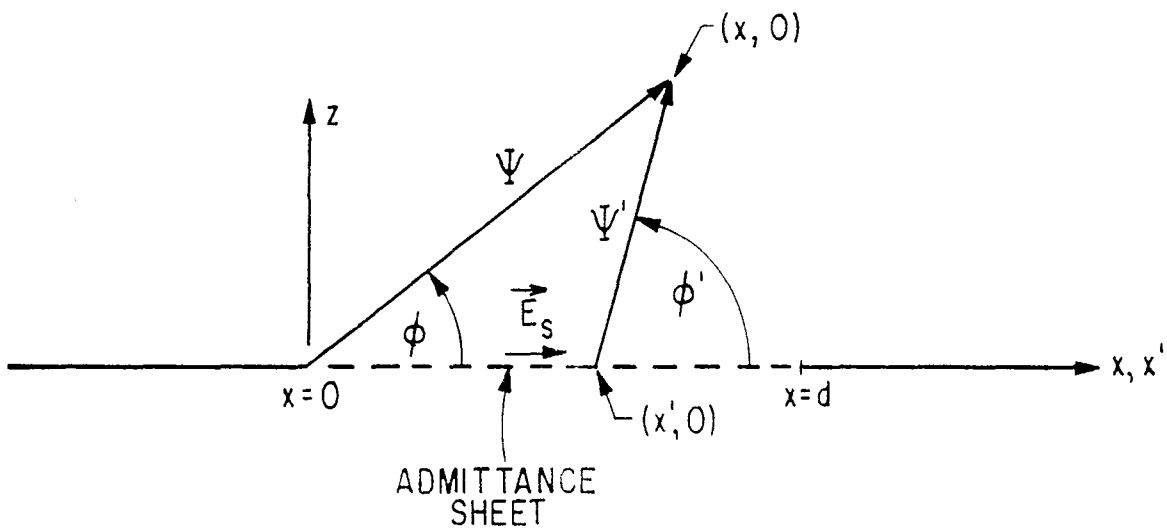
The purpose of this note is to calculate some of the characteristics of another type of admittance sheet terminating two parallel plates and the inductance and resistance values of the corresponding distributed LR termination. Specifically we consider the case of a sloped planar admittance sheet connecting the edges of semi-infinite perfectly conducting plates. As illustrated in figure 1A we also include perfectly conducting flanges (semi-infinite) connected to the edges of the parallel plates and coplanar with the admittance sheet. This allows us to calculate the currents on the admittance sheet as a boundary value problem with a plane boundary.

1. Capt Carl E. Baum, Sensor and Simulation Note 53, Admittance Sheets for Terminating High-Frequency Transmission Lines, April 1968.

2. R. W. Latham and K. S. H. Lee, Sensor and Simulation Note 68, Termination of Two Parallel Semi-Infinite Plates by a Matched Admittance Sheet, January 1969.



A. SLOPED TERMINATION WITH FLANGES



B. COORDINATES FOR CALCULATION (TWO DIMENSIONAL)

FIGURE I. ADMITTANCE SHEET TERMINATION

From the calculations in this note we find some of the effects associated with sloping the termination. These include how the parameters of the approximating LR termination should change and how closely the ideal surface current is approximated by the surface current associated with the incident electric field driving the approximate LR termination. While some practical cases of interest do not have the conducting flanges the calculations of the present note should apply at least qualitatively to such cases. Also the results of this note can be compared with the results in reference 2.

One of the reasons for considering a sloped termination is to make the incident wave arrive at the terminator at different times over the surface of the terminator. The reflections are then somewhat dispersed in time, or from another viewpoint the incident wave is not reflected directly back from the termination but is reflected at some other angle so that the reflected wave can in turn be reincident on the termination after reflecting off a conducting plane. The present boundary value problem does not calculate the reflections from an LR termination so this effect is not observed. Perhaps future notes can consider some idealized geometries in which such reflections can be calculated.

II. Boundary Value Problem

Now consider the boundary value problem which we will use to calculate the surface current density associated with the ideal admittance sheet. As illustrated in figure 1B the coordinates for the calculation are established with $z = 0$ as the plane of the admittance sheet and perfectly conducting flanges. In this problem we are concerned with the fields for $z > 0$ and the associated surface currents on the $z = 0$ plane. Note that we have a two-dimensional problem since our geometry and the incident fields are assumed independent of y . On the $z = 0$ plane the admittance sheet occupies the region $0 < x < d$ where³

$$d = \frac{h}{\sin(\xi)} \quad (1)$$

Note that ξ is the angle at which the admittance sheet and flanges are sloped with respect to the parallel plates as shown in figure 1A where we restrict $0 < \xi < \pi$.

There are actually two sets of coordinates. First there are the coordinates of the observer where the fields and current densities are to be calculated. These are the cartesian coordinates (x, y, z) and cylindrical coordinates (ρ, ϕ, z) related by

3. All units are rationalized MKSA.

$$\begin{aligned}x &= \Psi \cos(\phi) \\z &= \Psi \sin(\phi)\end{aligned}\tag{2}$$

The second set of coordinates involves the position on the admittance sheet and the position of the observer with respect to this other position on the admittance sheet. This position on the admittance sheet is needed as an integration variable in calculating the fields and surface current densities. We use x' for the coordinate on the admittance sheet instead of x . With this we have the cylindrical coordinates of the observer (with respect to $(x, z) = (x', 0)$) as $(\Psi', \phi', -y)$ given by

$$\begin{aligned}x - x' &= \Psi' \cos(\phi') \\z &= \Psi' \sin(\phi')\end{aligned}\tag{3}$$

See figure 1B for an illustration of these coordinate systems.

Another coordinate we use is ζ shown in figure 1A. The two parallel plates are at $\zeta = 0$ and $\zeta = h$. We use ζ to indicate positions on the admittance sheet in terms of the perpendicular distance from one of the plates (extended). For $z = 0$ ζ is related to x as

$$\zeta = \frac{h}{d} x = \sin(\xi)x\tag{4}$$

For purposes of normalization we sometimes use, for positions on the $z = 0$ plane,

$$\alpha \equiv \frac{\zeta}{h} = \sin(\xi) \frac{x}{h} = \frac{x}{d}\tag{5}$$

In setting up the boundary value problem we need to specify the tangential electric field on the admittance sheet as that given by the incident electric field. The incident wave is specified in the time domain as a step-function plane wave of the form

$$\vec{E}_{inc} = E_0 \vec{e}_1 u\left(t - \frac{\vec{r} \cdot \vec{e}_3}{c}\right)$$

$$\vec{H}_{inc} = \frac{E_0}{z_0} \vec{e}_2 u\left(t - \frac{\vec{r} \cdot \vec{e}_3}{c}\right) \quad (6)$$

where

$$z_0 \equiv \sqrt{\frac{\mu_0}{\epsilon_0}}, \quad c \equiv \frac{1}{\sqrt{\mu_0 \epsilon_0}} \quad (7)$$

and where E_0 is a convenient constant of dimensions V/m. The unit vectors for the coordinates are written \vec{e}_x, \vec{e}_y , etc. The three unit vectors for the incident wave (as in equation 6) can be written in terms of coordinate unit vectors as

$$\begin{aligned} \vec{e}_1 &= \sin(\xi) \vec{e}_x - \cos(\xi) \vec{e}_z \\ \vec{e}_2 &= \vec{e}_y \\ \vec{e}_3 &= \cos(\xi) \vec{e}_x + \sin(\xi) \vec{e}_z \end{aligned} \quad (8)$$

These unit vectors for the incident wave are related by

$$\vec{e}_1 \times \vec{e}_2 = \vec{e}_3, \quad \vec{e}_2 \times \vec{e}_3 = \vec{e}_1, \quad \vec{e}_3 \times \vec{e}_1 = \vec{e}_2 \quad (9)$$

For use with the step function we have the relation

$$\vec{r} \cdot \vec{e}_3 = x \cos(\xi) + z \sin(\xi) \quad (10)$$

On the admittance sheet the tangential electric field for $0 < x < d$ is given by

$$\begin{aligned} \vec{E}_s &= \left(\vec{E}_{inc} \Big|_{z=0} \cdot \vec{e}_x \right) \vec{e}_x + \left(\vec{E}_{inc} \Big|_{z=0} \cdot \vec{e}_y \right) \vec{e}_y \\ &= E_0 u\left(t - \frac{x}{c} \cos(\xi)\right) [(\vec{e}_1 \cdot \vec{e}_x) \vec{e}_x + (\vec{e}_1 \cdot \vec{e}_y) \vec{e}_y] \\ &= E_0 u\left(t - \frac{x}{c} \cos(\xi)\right) \sin(\xi) \vec{e}_x \end{aligned} \quad (11)$$

Thus the tangential electric field on the source has only an x component. Since we will be integrating over this field we use x' for the coordinate and also write the x component of the electric field on the whole $z = 0$ plane as

$$E'_x = E_0 \sin(\xi) u\left(t - \frac{x'}{c} \cos(\xi)\right) [u(x') - u(x' - d)] \quad (12)$$

Having the tangential field on the $z = 0$ plane with only an x component and only a function of x' and t we can write the expressions for the fields for $z > 0$ using the results of a previous note.⁴ From reference 4 equations 39 through 43 we have

$$E_x = - \int_{-\infty}^{\infty} \frac{\partial E'_x}{\partial t} * e'_{O_\phi} \frac{\sin(\phi')}{\Psi'} dx' \quad (13)$$

$$E_z = \int_{-\infty}^{\infty} \frac{\partial E'_x}{\partial t} * e'_{O_\phi} \frac{\cos(\phi')}{\Psi'} dx' \quad (14)$$

$$cB_y = Z_0 H_y = \int_{-\infty}^{\infty} \frac{\partial E'_x}{\partial t} * h'_O \frac{dx'}{\Psi'} \quad (15)$$

where

$$e'_{O_\phi} = - \frac{1}{\pi} \frac{ct}{\Psi'} \left[\left(\frac{ct}{\Psi'} \right)^2 - 1 \right]^{-1/2} u\left(t - \frac{\Psi'}{c}\right) \quad (16)$$

$$h'_O = \frac{1}{\pi} \left[\left(\frac{ct}{\Psi'} \right)^2 - 1 \right]^{-1/2} u\left(t - \frac{\Psi'}{c}\right) \quad (17)$$

and where * indicates the convolution integral with respect to time. While we are not going to explicitly calculate and graph these field components we will use the expressions for the magnetic field to calculate the surface current density on the $z = 0$ plane associated with this magnetic field.

4. Capt Carl E. Baum, Sensor and Simulation Note 66, A Simplified Two-Dimensional Model for the Fields Above the Distributed-Source Surface Transmission Line, December 1968.

III. Currents Produced by Incident Electric Field in an Inductive-Resistive Termination

For comparison with the surface current density associated with an ideal admittance-sheet termination we first consider the surface current density associated with a termination whose surface impedance is given by the series combination of a resistance R_s and an inductance L_s . The surface admittance of this LR sheet is then

$$Y'_s = [sL_s + R_s]^{-1} \quad (18)$$

where s is the Laplace transform variable (with respect to time). Now for $0 < x < d$ the incident electric field on the termination from equation 11 has only an x component given by

$$E_{s_x} = E_o \sin(\xi) u\left(t - \frac{x}{c} \cos(\xi)\right) \quad (19)$$

Associated with this electric field and the surface admittance in equation 18 there is a surface current density for $0 < x < d$ with only an x component given by

$$J_{s_o} = \frac{E_o \sin(\xi)}{R_s} \left[1 - e^{-\left(t - \frac{x}{c} \cos(\xi)\right) \frac{R_s}{L_s}} \right] u\left(t - \frac{x}{c} \cos(\xi)\right) \quad (20)$$

Note that we are not including any reflections, etc. in calculating J_{s_o} ; this surface current density is used for comparison with the surface current density on an ideal admittance sheet to see how close the two can be brought to having the same amplitude and time history.

Now as $t \rightarrow \infty$ we want $J_{s_o} \rightarrow E_o/Z_o$ to terminate the parallel plate transmission line at late times (or low frequencies). Note that for low frequencies the magnetic field for $z > 0$ will be negligible compared to the magnetic field between the parallel plates. Thus we constrain

$$R_s \equiv Z_o \sin(\xi) \quad (21)$$

For convenience define

$$t_s \equiv \frac{L_s}{R_s} = \frac{1}{\sin(\xi)} \frac{L_s}{Z_0}, \quad j_{s_0} \equiv \frac{Z_0}{E_0} J_{s_0} \quad (22)$$

so that the normalized surface current density associated with the LR terminator and incident electric field is

$$j_{s_0} = \left[1 - e^{-\left(t - \frac{x}{c} \cos(\xi)\right) \frac{1}{t_s}} \right] u\left(t - \frac{x}{c} \cos(\xi)\right) \quad (23)$$

For convenience we define two normalized retarded times for use with surface current densities on the $z = 0$ plane as

$$\begin{aligned} \tau_\zeta^* &\equiv \frac{ct - x \cos(\xi)}{\zeta} = \frac{ct}{\zeta} - \cot(\xi) \\ &= \frac{1}{\sin(\xi)} \left[\frac{ct}{x} - \cos(\xi) \right] \end{aligned} \quad (24)$$

and

$$\tau_h^* \equiv \frac{ct - x \cos(\xi)}{h} = \frac{ct}{h} - \alpha \cot(\xi) \quad (25)$$

The first normalized retarded time (equation 24) will be used when we are only considering the effects associated with the end of the admittance sheet at $x = 0$. The second normalized retarded time will be used when the effects associated with both ends of the admittance sheet are included.

Corresponding to the two normalized retarded times we define two characteristic times as

$$t_\zeta \equiv \frac{\zeta}{c}, \quad t_h \equiv \frac{h}{c} \quad (26)$$

Also define two dimensionless parameters related to the surface inductance as

$$\beta_{\zeta} \equiv \frac{t_s}{t_{\zeta}} = \frac{c}{\zeta} \frac{L_s}{R_s} = \frac{1}{\sin(\xi)} \frac{c}{\zeta} \frac{L_s}{Z_0} \quad (27)$$

$$\beta_h \equiv \frac{t_s}{t_h} = \frac{c}{h} \frac{L_s}{R_s} = \frac{1}{\sin(\xi)} \frac{c}{h} \frac{L_s}{Z_0}$$

Then j_{s_0} (for $0 < x < d$) can be written in the two forms as

$$j_{s_0} = \left[1 - e^{-\frac{\tau_{\zeta}^*}{\beta_{\zeta}}} \right] u(\tau_{\zeta}^*) \quad (28)$$

and

$$j_{s_0} = \left[1 - e^{-\frac{\tau_h^*}{\beta_h}} \right] u(\tau_h^*) \quad (29)$$

These are the forms we will use for later comparison.

IV. Currents Associated with Ideal Termination

In equation 12 we have the tangential electric field on the admittance sheet; note that it can be split into two terms as

$$E'_1 = E_0 \sin(\xi) u\left(t - \frac{x'}{c} \cos(\xi)\right) u(x') \quad (30)$$

$$E'_2 = -E_0 \sin(\xi) u\left(t - \frac{x'}{c} \cos(\xi)\right) u(x' - d)$$

where

$$E'_x = E'_1 + E'_2 \quad (31)$$

Note that we will normally think of ξ in the range $0 < \xi \leq \pi/2$. For positions near $x = 0$ the effect of E'_1 will be noticed first in time with the effect of E'_2 coming in later.

A. Effect of the end of the admittance sheet at $x = 0$

Now consider the effect of E_1' . The results will apply for times before any effects associated with the end of the admittance sheet at $x = d$ (or $z = h$) can propagate to the position of interest on the admittance sheet. We need the surface current density on the $z = 0$ plane associated with E_1' . We get this from the magnetic field in equation 15. Defining normalized surface current densities as

$$j_{s_1} \equiv - \left. \frac{Z_0 H_y}{E_0} \right|_{\phi=0+}$$

$$j_{s_2} \equiv - \left. \frac{Z_0 H_y}{E_0} \right|_{\phi=\pi-}$$
(32)

we have for $x > 0$

$$j_{s_1} = - \frac{\sin(\xi)}{\pi} \int_0^\infty \delta\left(t - \frac{x'}{c} \cos(\xi)\right) * \left\{ \left[\left(\frac{ct}{|x - x'|} \right)^2 - 1 \right]^{-1/2} u\left(t - \frac{|x - x'|}{c}\right) \right\} \frac{dx'}{|x - x'|}$$
(33)

and for $x < 0$

$$j_{s_2} = - \frac{\sin(\xi)}{\pi} \int_0^\infty \delta\left(t - \frac{x'}{c} \cos(\xi)\right) * \left\{ \left[\left(\frac{ct}{x - x'} \right)^2 - 1 \right]^{-1/2} u\left(t + \frac{x - x'}{c}\right) \right\} \frac{dx'}{x' - x}$$
(34)

Performing the convolution integrals gives

$$j_{s_1} = - \frac{\sin(\xi)}{\pi} \int_0^{\infty} \left[\left(\frac{ct - x' \cos(\xi)}{|x - x'|} \right)^2 - 1 \right]^{-1/2} \cdot u(ct - x' \cos(\xi) - |x - x'|) \frac{dx'}{|x - x'|} \quad (35)$$

and

$$j_{s_2} = - \frac{\sin(\xi)}{\pi} \int_0^{\infty} \left[\left(\frac{ct - x' \cos(\xi)}{-x + x'} \right)^2 - 1 \right]^{-1/2} \cdot u(ct - x' \cos(\xi) + x - x') \frac{dx'}{x' - x} \quad (36)$$

With the chosen sign convention j_{s_1} and j_{s_2} are taken positive in the $+x$ direction.

For convenience define

$$\tau \equiv \frac{ct}{|x|} \quad (37)$$

Consider first j_{s_2} which we can write as

$$\begin{aligned} j_{s_2} &= - \frac{\sin(\xi)}{\pi} u(ct+x) \int_0^{\frac{ct+x}{1+\cos(\xi)}} \left[(ct-x'\cos(\xi))^2 - (x'-x)^2 \right]^{-1/2} dx' \\ &= - \frac{\sin(\xi)}{\pi} u(\tau-1) \int_0^{-x \frac{\tau-1}{1+\cos(\xi)}} [-\sin^2(\xi)x'^2 \\ &\quad + 2x(1+\tau\cos(\xi))x' + x^2(\tau^2-1)]^{-1/2} dx' \end{aligned} \quad (38)$$

From a standard reference⁵ we have

$$\begin{aligned}
 j_{s_2} &= - \frac{\sin(\xi)u(\tau-1)}{\pi} \frac{-1}{\sin(\xi)} \arcsin \left[\frac{\sin^2(\xi) \frac{x'}{x} - 1 - \tau \cos(\xi)}{\tau + \cos(\xi)} \right] \Bigg|_{-x \frac{\tau-1}{1+\cos(\xi)}}^0 \\
 &= - \frac{u(\tau-1)}{\pi} \left\{ \frac{\pi}{2} - \arcsin \left[\frac{1+\tau \cos(\xi)}{\tau + \cos(\xi)} \right] \right\} \\
 &= - \frac{u(\tau-1)}{\pi} \arccos \left[\frac{1+\tau \cos(\xi)}{\tau + \cos(\xi)} \right] \quad (39)
 \end{aligned}$$

Thus we have the surface current density on the $z = 0$ plane for $x < 0$ and for a semi-infinite admittance sheet, i.e. including only E_1 . We will later use this result to find the surface current density on the admittance sheet associated with E_2 .

Now consider j_{s_1} which we can write as

$$\begin{aligned}
 j_{s_1} &= - \frac{\sin(\xi)}{\pi} u(\tau - x \cos(\xi)) \int_{x_0}^{x_1} [(ct - x' \cos(\xi))^2 - (x' - x)^2]^{-1/2} dx' \\
 &= - \frac{\sin(\xi)}{\pi} u(\tau - \cos(\xi)) \int_{x_0}^{x_1} [-\sin^2(\xi) x'^2 \\
 &\quad + 2x(1 - \tau \cos(\xi)) + x^2(\tau^2 - 1)]^{-1/2} dx' \quad (40)
 \end{aligned}$$

where the limits on the integral are

5. H. B. Dwight, Tables of Integrals and Other Mathematical Data, 4th ed., Macmillan, 1965, eqn. 380.001.

$$x_1 = \frac{ct + x}{1 + \cos(\xi)} = x \frac{\tau + 1}{1 + \cos(\xi)} \quad (41)$$

$$x_0 = \max\left[0, \frac{x - ct}{1 - \cos(\xi)}\right] = \max\left[0, x \frac{1 - \tau}{1 - \cos(\xi)}\right]$$

Thus we have two cases to consider. Note we restrict $0 < \xi \leq \pi/2$.

First let $\cos(\xi) < \tau < 1$ so that using reference 5 j_{s_1} can be written as

$$j_{s_1} = - \frac{\sin(\xi)u(\tau - \cos(\xi))}{\pi} \frac{-1}{\sin(\xi)} \cdot \arcsin\left[\frac{-\sin^2(\xi)\frac{x'}{x} + 1 - \tau\cos(\xi)}{\tau - \cos(\xi)}\right] \Bigg|_{x \frac{1-\tau}{1-\cos(\xi)}}^{x \frac{\tau+1}{1+\cos(\xi)}} = -u(\tau - \cos(\xi)) \quad (42)$$

This result applies for all $\tau < 1$. Second let $\tau > 1$ giving

$$j_{s_1} = - \frac{\sin(\xi)u(\tau - 1)}{\pi} \frac{-1}{\sin(\xi)} \arcsin\left[\frac{-\sin^2(\xi)\frac{x'}{x} + 1 - \tau\cos(\xi)}{\tau - \cos(\xi)}\right] \Bigg|_0^{x \frac{\tau+1}{1+\cos(\xi)}} = - \frac{u(\tau - 1)}{\pi} \left[\frac{\pi}{2} + \arcsin\left[\frac{1 - \tau\cos(\xi)}{\tau - \cos(\xi)}\right] \right] = -u(\tau - 1) \left[1 - \frac{1}{\pi} \arccos\left[\frac{1 - \tau\cos(\xi)}{\tau - \cos(\xi)}\right] \right] \quad (43)$$

We can write one equation, combining the results of equations 42 and 43, to give a result valid for all τ as

$$j_{s_1} = -u(\tau - \cos(\xi)) + \frac{u(\tau - 1)}{\pi} \arccos\left[\frac{1 - \tau \cos(\xi)}{\tau - \cos(\xi)}\right] \quad (44)$$

Now the surface current density (in the +x direction) required on an ideal admittance sheet is given by

$$J_s = H_Y \Big|_{z=0-} - H_Y \Big|_{z=0+} \quad (45)$$

Thus for times before the effect of the end of the admittance sheet at $x = d$ is seen we have a surface current density of the form

$$J_s = \frac{E_0}{Z_0} \left[u(\tau - \cos(\xi)) + j_{s_1} \right] \quad (46)$$

From this we define a normalized surface current density for $x > 0$ as

$$\begin{aligned} j_{s_3} &\equiv u(\tau - \cos(\xi)) + j_{s_1} \\ &= \frac{u(\tau - 1)}{\pi} \arccos\left[\frac{1 - \tau \cos(\xi)}{\tau - \cos(\xi)}\right] \end{aligned} \quad (47)$$

In terms of the normalized retarded time τ_ζ^* appropriate to this case we have

$$\tau = \frac{ct}{x} = \sin(\xi)\tau_\zeta^* + \cos(\xi) \quad (48)$$

giving

$$j_{s_3} = \frac{1}{\pi} u\left(\tau_\zeta^* - \frac{1 - \cos(\xi)}{\sin(\xi)}\right) \arccos\left[\frac{\sin(\xi) - \tau_\zeta^* \cos(\xi)}{\tau_\zeta^*}\right] \quad (49)$$

Note the interesting limiting case for small ξ as

$$\lim_{\xi \rightarrow 0} j_{s_3} = u(\tau_\zeta^*) \quad (50)$$

where ξ is kept a constant in taking the limit. Note in this limit that $x \rightarrow \infty$. Another interesting limit is the case for large τ_ξ^* which is given by

$$\lim_{\tau_\xi^* \rightarrow \infty} j_{s3} = 1 - \frac{\xi}{\pi} \quad (51)$$

Note that this limit is not 1; an additional term associated with the end of the admittance sheet at $x = d$ is needed to make the limit 1.

In figure 2 we have j_{s3} plotted as a function of τ_ξ^* for various values of ξ in the range $0 < 2\xi/\pi \leq 1$. Note that as $\xi \rightarrow 0$ the j_{s3} waveforms shift toward the left and top of the graphs. Basically this means that for small ξ the undesirable features of j_{s3} shift to earlier times or higher frequencies. Also for small ξ the late time asymptote shifts up toward 1. Now one could define an ideal j_{s3} as a unit step function; then one would only need R_s to make j_{s0} the same as j_{s3} . Since j_{s3} is not a step function we can choose β_ξ (and thus L_s) in equations 27 and 28 in a manner which makes j_{s0} best approximate j_{s3} in some sense. In figure 2 we have included j_{s0} for various values of β_ξ for comparison with j_{s3} . Then for a given value of ξ one can choose a value of β_ξ which makes the LR termination "best" approximate the required termination as given by j_{s3} . Note that these results only include the effects associated with one end of the admittance sheet. We now go on to consider the case with both ends included.

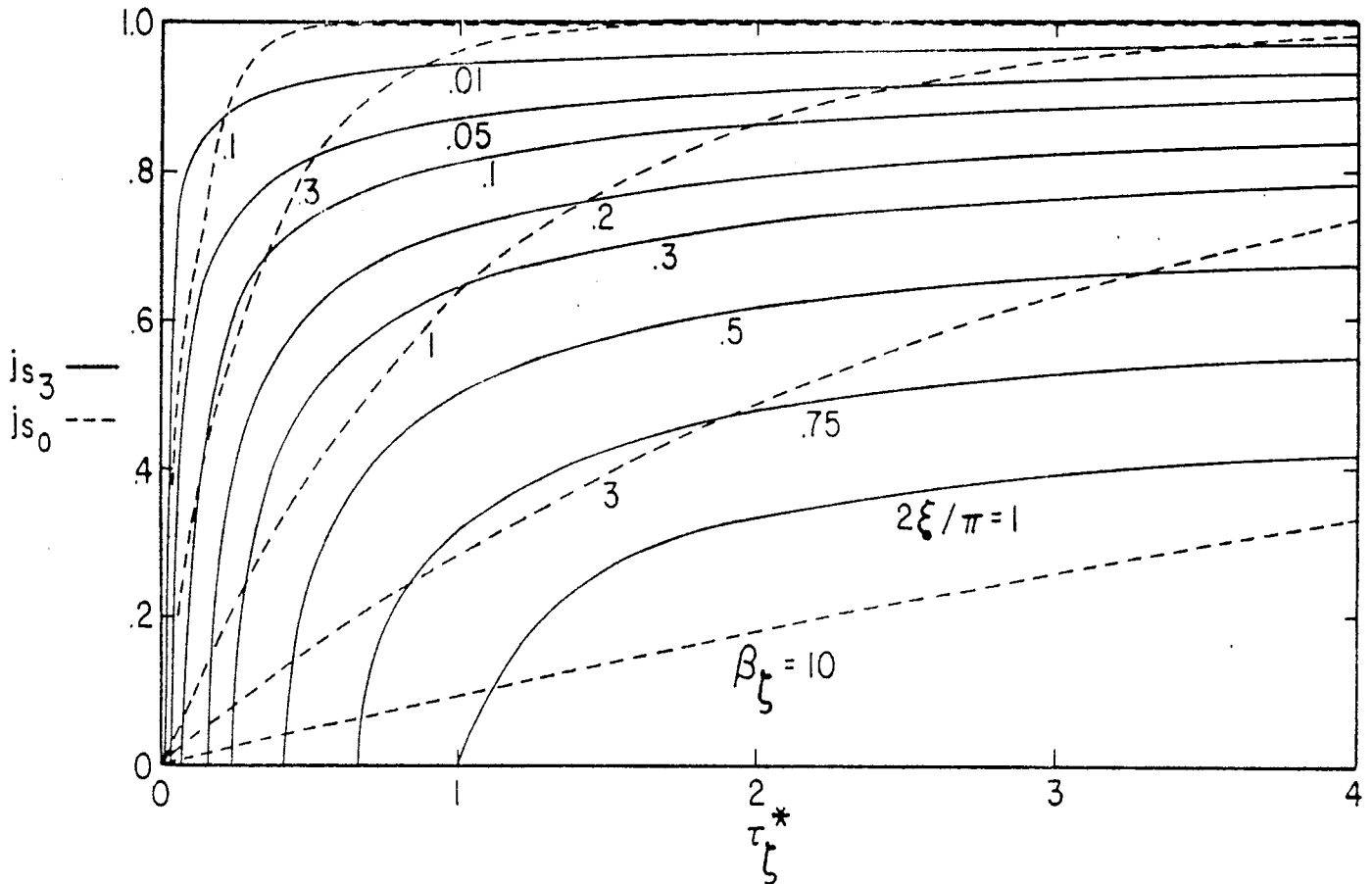
B. Effects of both ends of the admittance sheet

The effect of including E_2^i in calculating the surface current densities can be easily obtained from the results for E_1^i by noting that E_2^i can be obtained from E_1^i by a change in sign, a shift in x by an amount d , and a time delay $d \cos(\xi)/c$. The results for j_{s1} and j_{s2} can then be used by replacing ct by $ct - d \cos(\xi)$ and replacing $|x|$ by $|x - d|$. Then on the ideal admittance sheet we have a surface current density from equation 45 for $0 < x < d$ given by

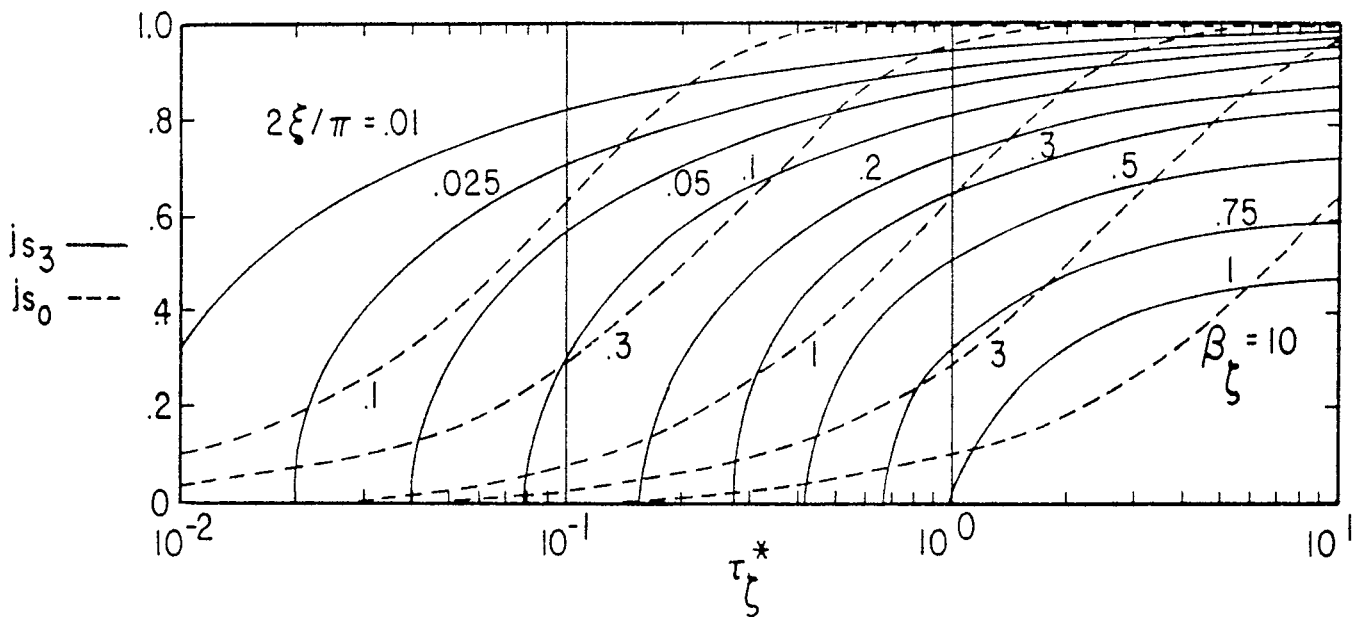
$$J_s = \frac{E_0}{Z_0} \left[u(\tau - \cos(\xi)) + j_{s1} + j_{s2}' \right] \quad (52)$$

where j_{s2}' is obtained from j_{s2} with the substitution mentioned above as

$$j_{s2}' = \frac{u(\tau' - 1)}{\pi} \arccos \left[\frac{1 + \tau' \cos(\xi)}{\tau' + \cos(\xi)} \right] \quad (53)$$



A. i_{s3} FOR VARIOUS $2\xi/\pi$ PLUS i_{s0} FOR VARIOUS β_ζ FOR COMPARISON



B. i_{s3} FOR VARIOUS $2\xi/\pi$ PLUS i_{s0} FOR VARIOUS β_ζ FOR COMPARISON

FIGURE 2. SURFACE CURRENT DENSITY FOR THE CASE THAT ONLY THE END OF THE ADMITTANCE SHEET AT THE TOP PLATE ($x=0$) IS CONSIDERED

where

$$\tau' \equiv \frac{ct - d \cos(\xi)}{|x - d|}, \quad \tau = \frac{ct}{|x|} \quad (54)$$

In normalized form we define

$$\begin{aligned} j_{s_4} &= u(\tau - \cos(\xi)) + j_{s_1} + j'_{s_2} \\ &= j_{s_3} + j'_{s_2} \end{aligned} \quad (55)$$

In terms of the normalized retarded time τ_h^* and α (from equation 5) we have (for $0 < x < d$)

$$\tau = \frac{ct}{x} = \frac{h}{x} \left[\tau_h^* + \frac{x}{h} \cos(\xi) \right] = \frac{\sin(\xi)}{\alpha} \tau_h^* + \cos(\xi) \quad (56)$$

$$\begin{aligned} \tau' &= \frac{ct - d \cos(\xi)}{d - x} = \frac{h}{d - x} \left[\tau_h^* + \frac{x}{h} \cos(\xi) - \frac{d}{h} \cos(\xi) \right] \\ &= \frac{\sin(\xi)}{1 - \alpha} \tau_h^* - \cos(\xi) \end{aligned} \quad (57)$$

In terms of τ_h^* we can write

$$\begin{aligned} j_{s_4} &= \frac{1}{\pi} u\left(\tau_h^* - \alpha \frac{1 - \cos(\xi)}{\sin(\xi)}\right) \arccos \left[\frac{\alpha \sin(\xi) - \tau_h^* \cos(\xi)}{\tau_h^*} \right] \\ &\quad + \frac{1}{\pi} u\left(\tau_h^* - (1 - \alpha) \frac{1 + \cos(\xi)}{\sin(\xi)}\right) \arccos \left[\frac{(1 - \alpha) \sin(\xi) + \tau_h^* \cos(\xi)}{\tau_h^*} \right] \end{aligned} \quad (58)$$

Note that for small ξ we have

$$\lim_{\xi \rightarrow 0} j_{s_4} = u(\tau_h^*) \quad (59)$$

where α is kept a constant in taking the limit. Note that in this limit we also have $d \rightarrow \infty$ and $x \rightarrow \infty$. Also we have the limiting case for large τ_h^* as

$$\lim_{\tau_h^* \rightarrow \infty} j_{s_4} = 1 \quad (60)$$

Comparing this result to that in equation 51, note that including both ends of the admittance sheet makes the late time limit 1, a contribution of ξ/π coming from the end at $x = d$.

In figures 3 through 9 j_{s_4} is plotted as a function of τ_h^* for various values of ξ ranging from $\pi/2$ down to $.01 \pi/2$, and for various values of α ($= \zeta/h$) with $0 < \alpha < 1$. Note that as $\xi \rightarrow 0$ all the j_{s_4} waveforms tend toward unit-step functions, i.e. they rise close to unity sooner. However also note that as $\xi \rightarrow 0$ the influence of the end of the admittance sheet at $x = d$ appears later and later in time after the initial rise. As $\xi \rightarrow 0$ a plateau of $1 - \xi/\pi$ is rapidly approached by j_{s_4} (like j_{s_3} in equation 51). The rest of the rise of j_{s_4} to 1 occurs after the arrival of the signal from $x = d$; on the last several of the figures this remaining portion of the rise of j_{s_4} has not begun (except at $\alpha = 1$) in the time scale of the graphs.

Also included in figures 3 through 9 are curves of j_{s_0} (from equation 29) as a function of τ_h^* for various values of β_h . These are for comparison with j_{s_4} . The value of β_h needed to make j_{s_0} best approximate j_{s_4} (in some sense) decreases as $\xi \rightarrow 0$. For any given value of ξ one can try to pick some value of β_h which makes j_{s_0} best approximate j_{s_4} over the entire admittance sheet ($0 < \alpha < 1$), or one might even make β_h take on different values at different positions on the admittance sheet.

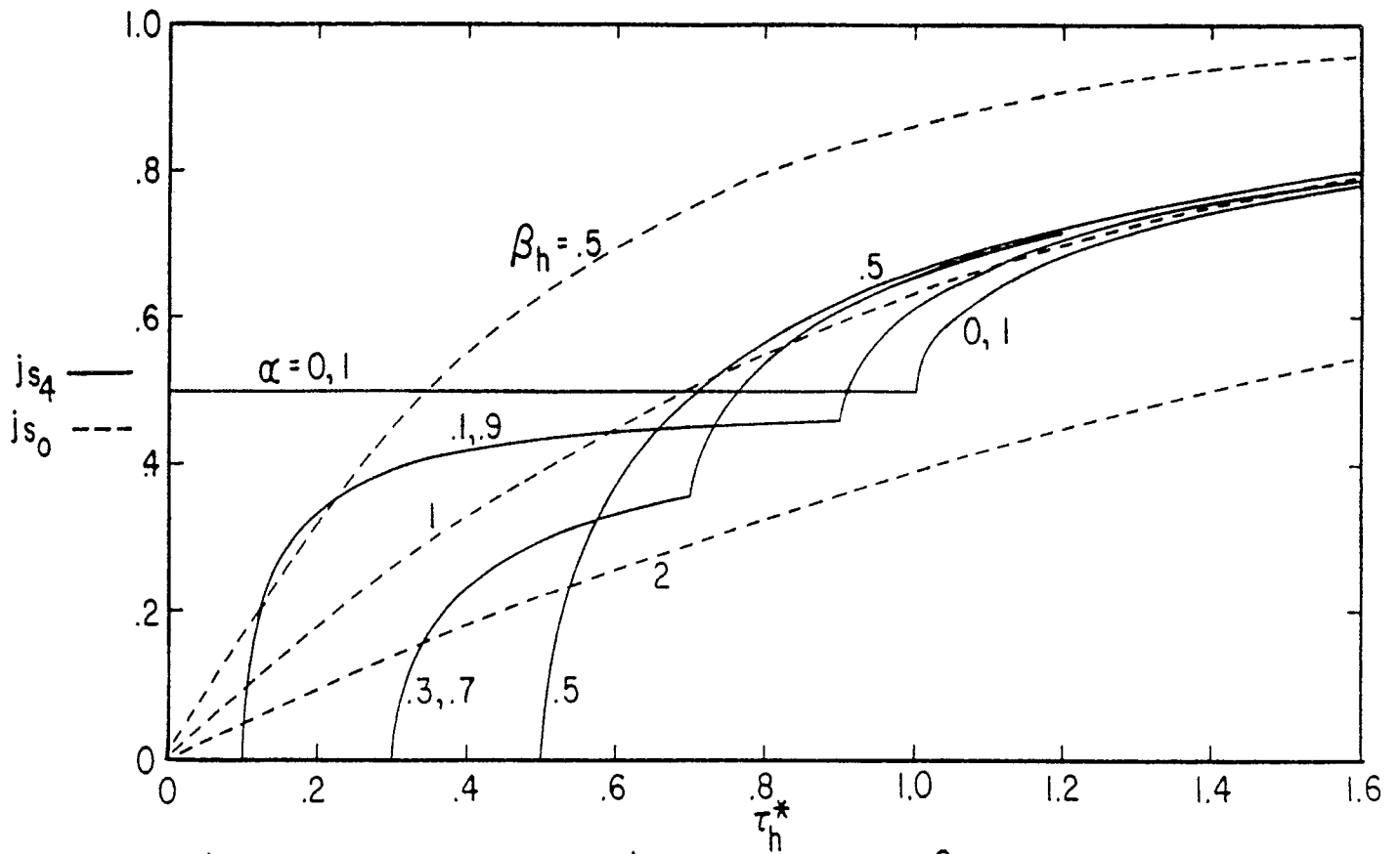
V. Summary

In this note we have considered the effect of sloping a distributed termination plus conducting flanges at the end of an infinitely wide parallel-plate transmission line. While we are mainly interested in a case without flanges, the present results should apply in a qualitative manner. Note that as $\xi \rightarrow 0$ the present case with flanges tends to a case in which there are no flanges (in the limit), i.e. one flange merges with one of the transmission-line boundaries and the other tends toward an extension of the other transmission-line boundary, thereby tending toward a continuous ground plane.

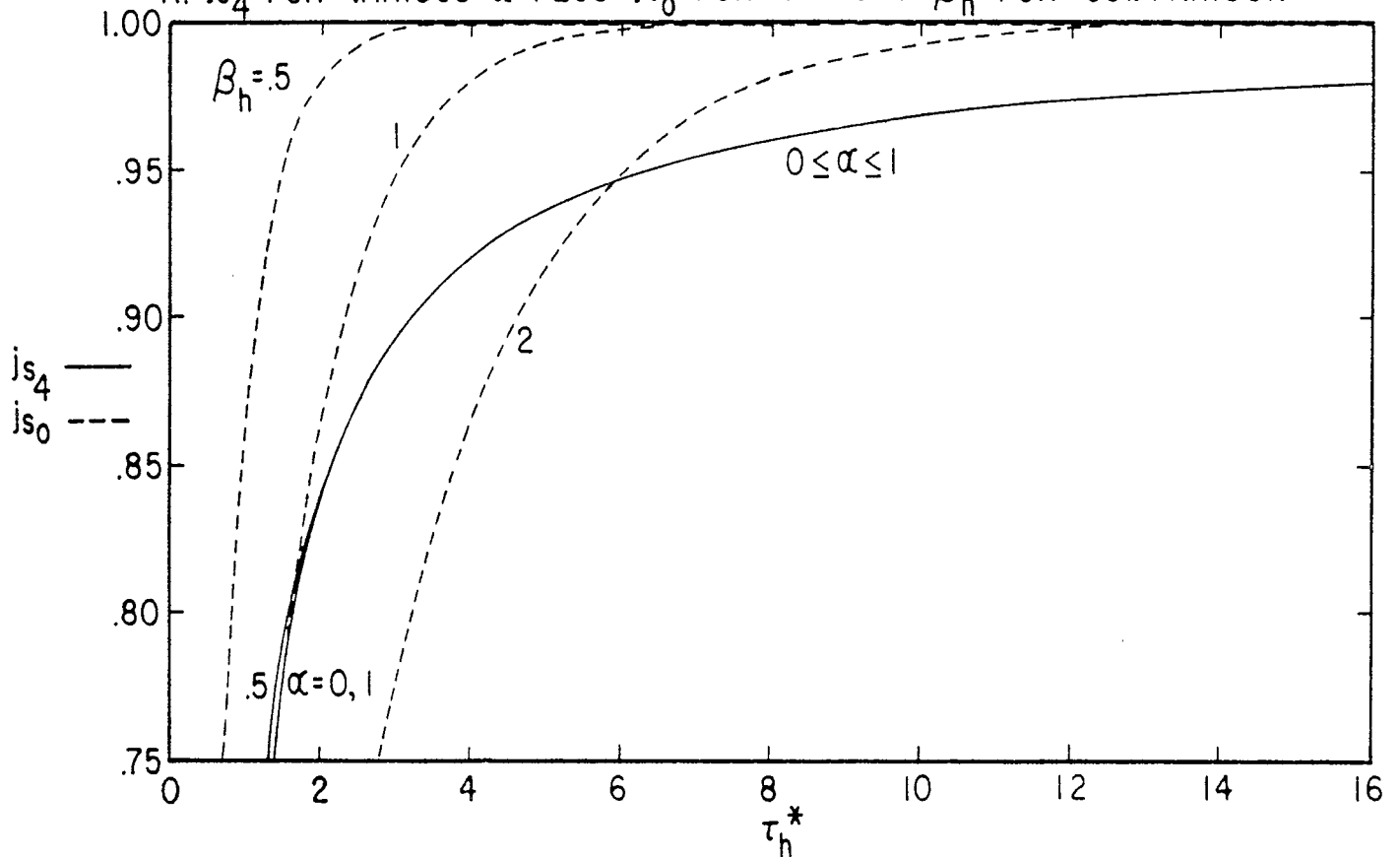
One of the advantages to be gained in sloping the termination is that the required current in the termination more quickly

approaches (for a step-function incident wave) the late-time limiting current. Roughly speaking this occurs because the disturbance from the end of one of the parallel plates can reach a typical position on the termination more quickly after the arrival of the incident wave at that position. There is some contribution from the end of the termination reached last by the incident wave but as $\xi \rightarrow 0$ this contribution is small. As $\xi \rightarrow 0$ the required value of $\beta_h \rightarrow 0$ also. Since L_s is proportional to $\beta_h \sin(\xi)$ for a given h , then as $\xi \rightarrow 0$ we also have $L_s \rightarrow 0$, reducing the required surface inductance in the termination.

We would like to thank Sgt. Richard T. Clark and A2C Robert N. Marks of AFWL and Mr. Joe P. Martinez of Dikewood for the numerical calculations and graphs.

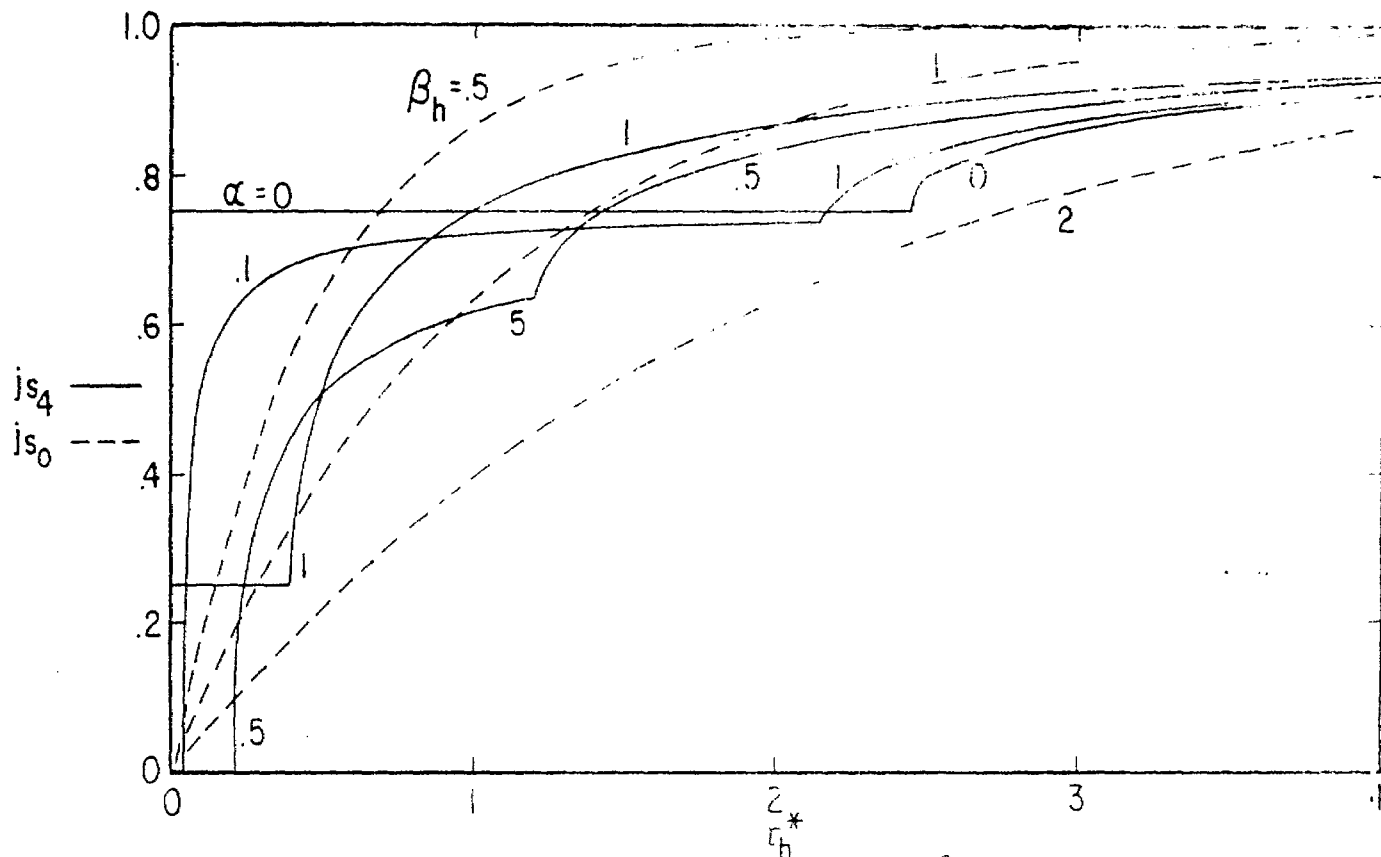


A. j_{s_4} FOR VARIOUS α PLUS j_{s_0} FOR VARIOUS β_h FOR COMPARISON

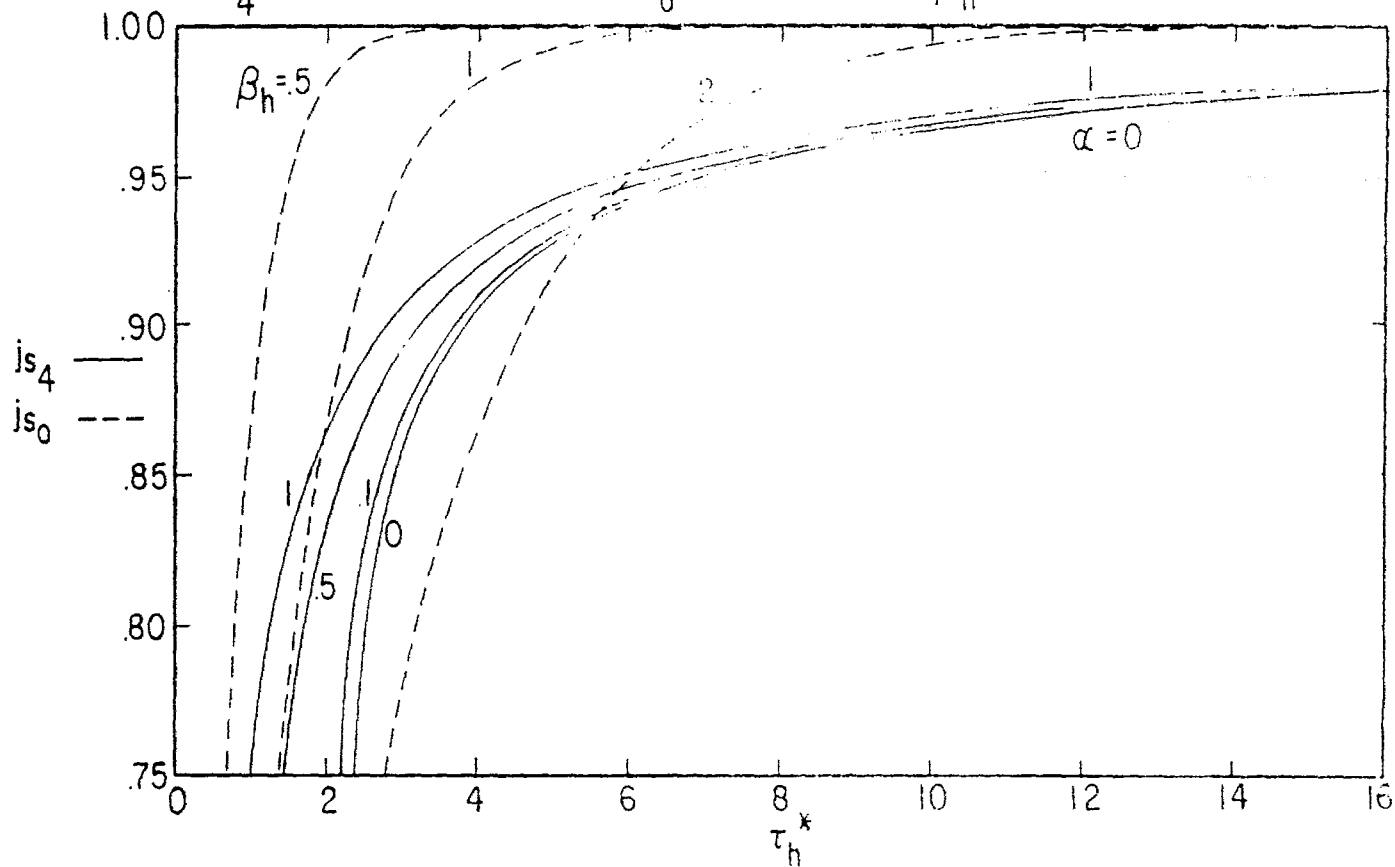


B. SCALES OF A CHANGED TO SHOW LATE-TIME BEHAVIOR

FIGURE 3. SURFACE CURRENT DENSITY INCLUDING BOTH ENDS OF THE ADMITTANCE SHEET: $2\xi/\pi = 1$

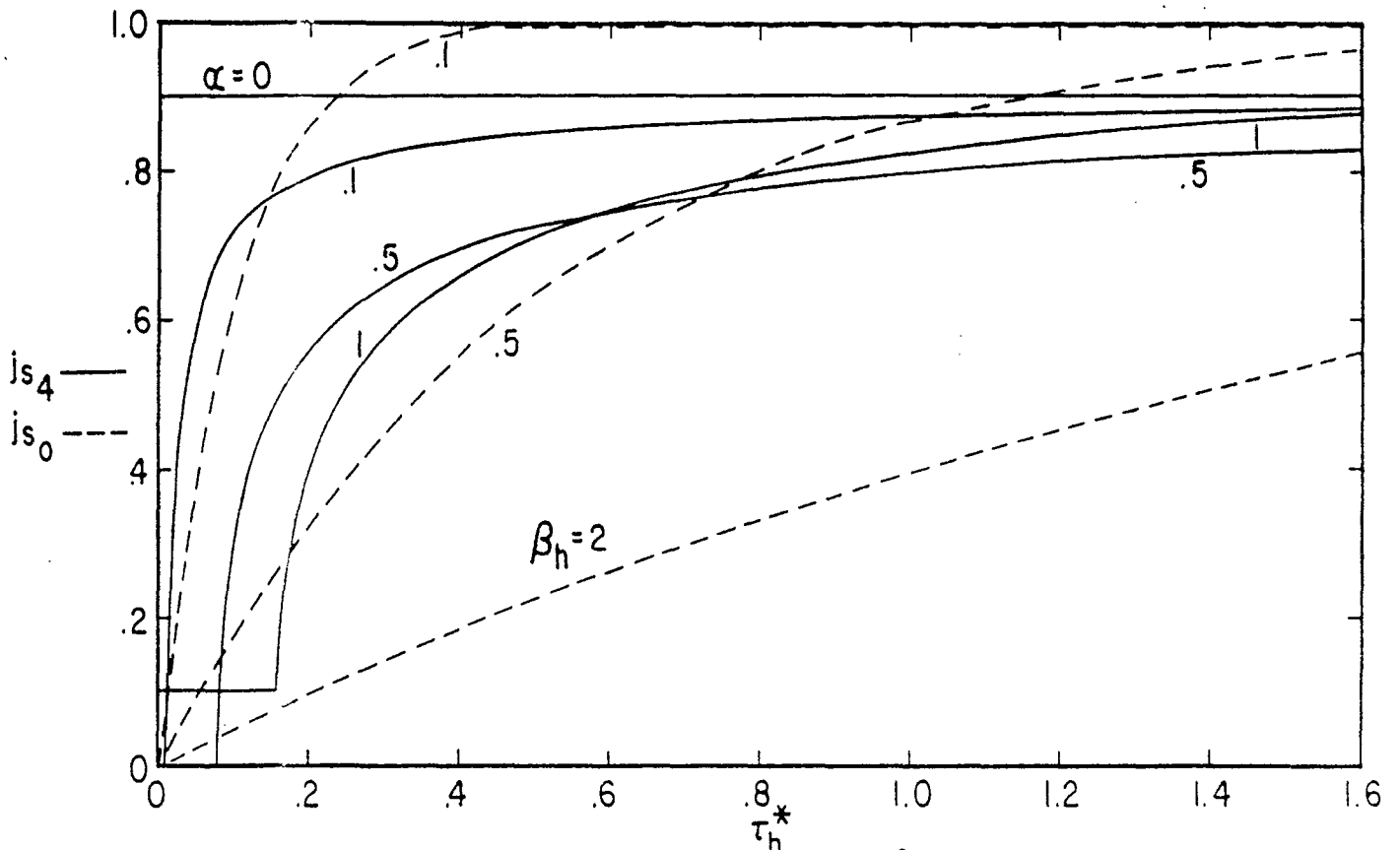


A. js_4 FOR VARIOUS α PLUS js_0 FOR VARIOUS β_h FOR COMPARISON

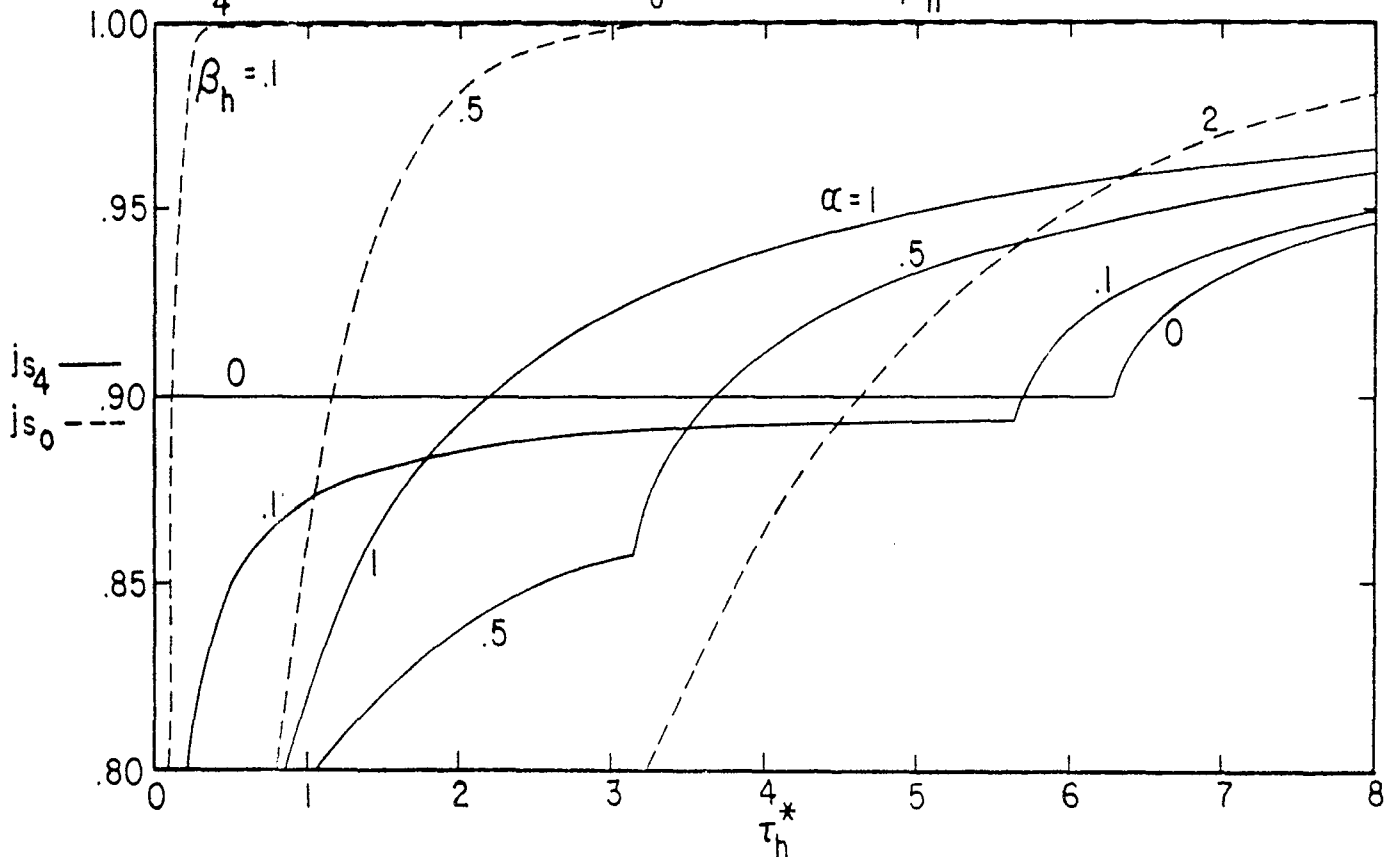


B. SCALES OF A CHANGED TO SHOW LATE-TIME BEHAVIOR

FIGURE 4. SURFACE CURRENT DENSITY INCLUDING BOTH ENDS OF THE ADMITTANCE SHEET : $2\xi/\pi = .5$

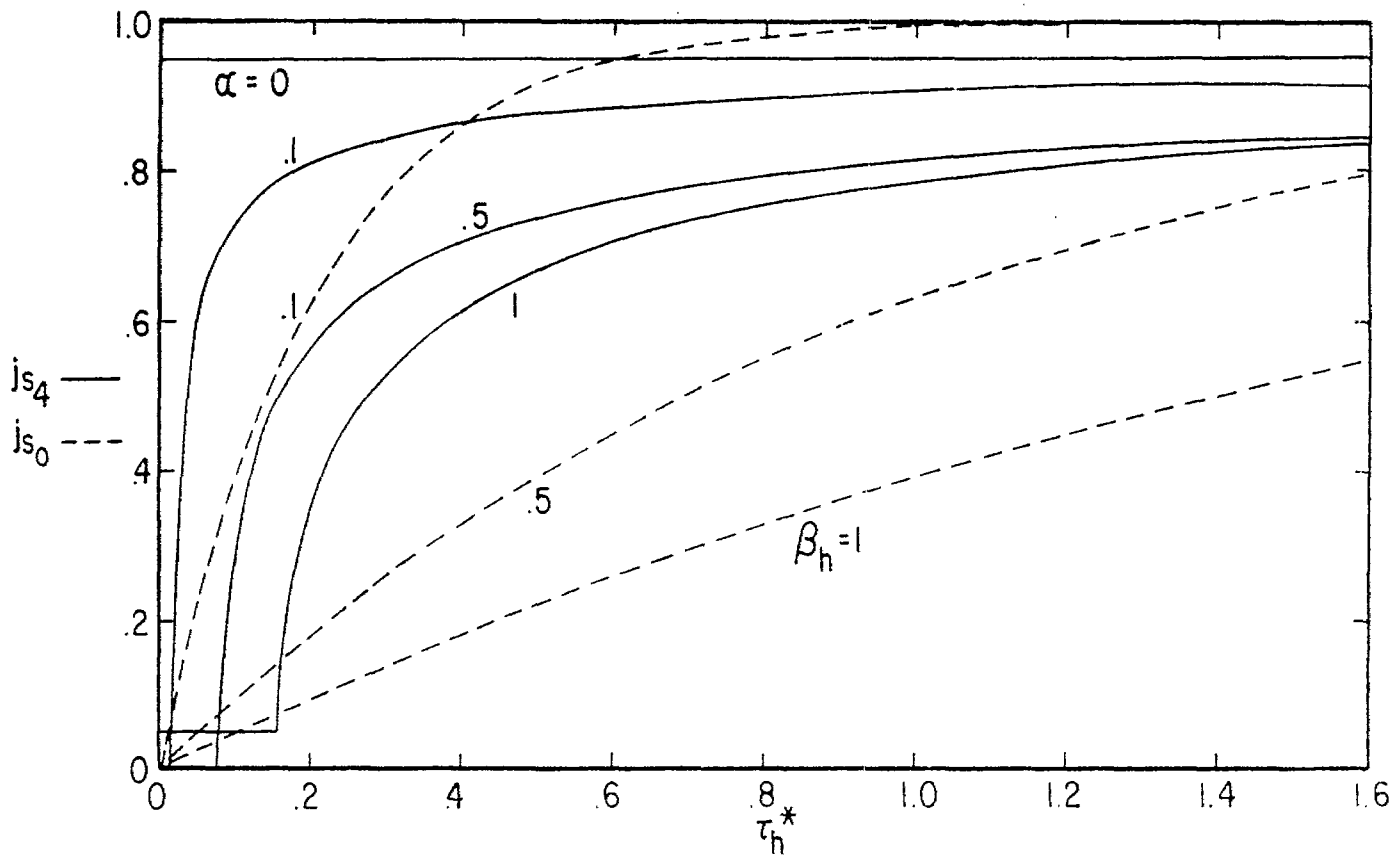


A. j_{s4} FOR VARIOUS α PLUS j_{s0} FOR VARIOUS β_h FOR COMPARISON

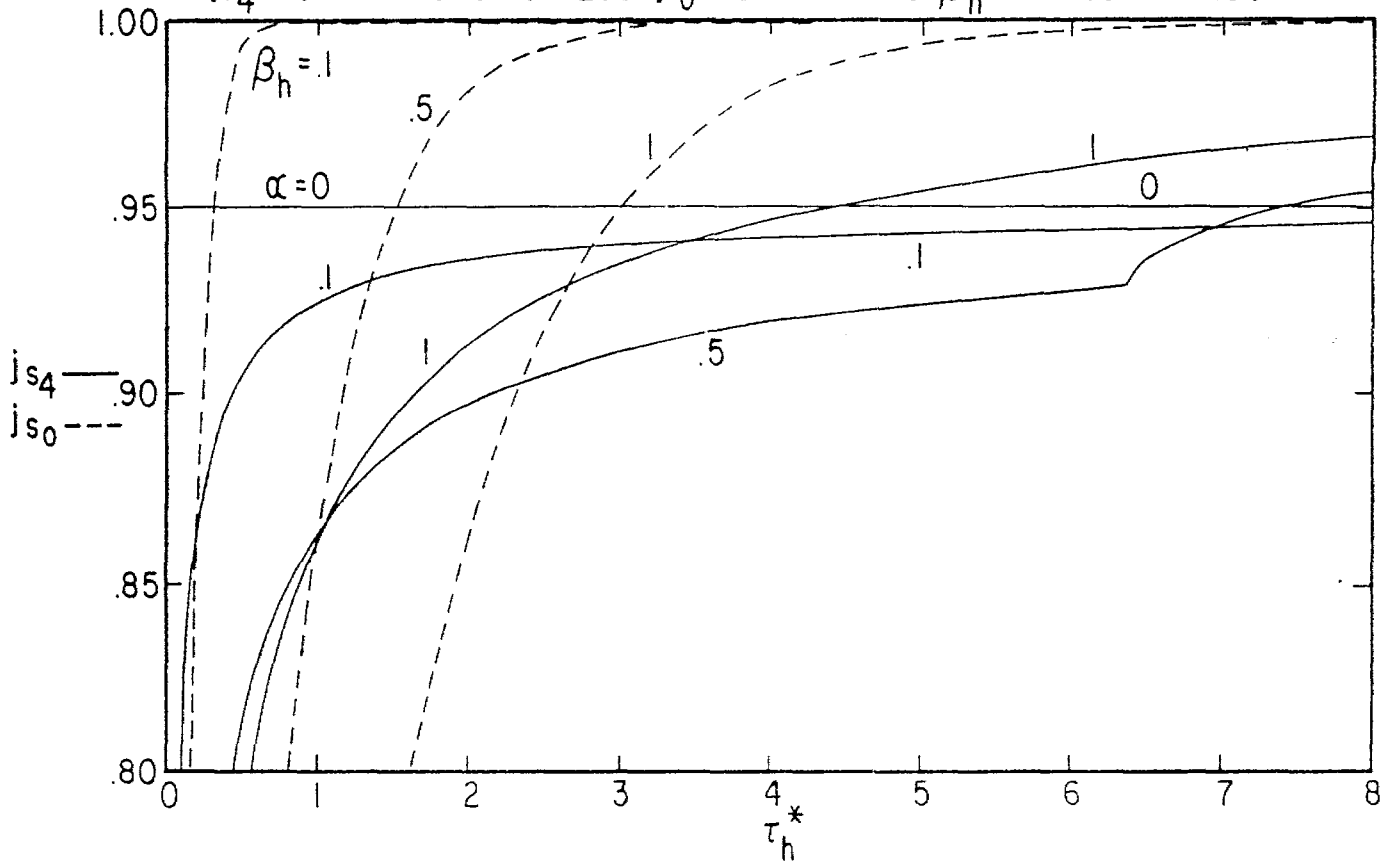


B. SCALES OF A CHANGED TO SHOW LATE-TIME BEHAVIOR

FIGURE 5. SURFACE CURRENT DENSITY INCLUDING BOTH ENDS OF THE ADMITTANCE SHEET: $2\xi/\pi = .2$

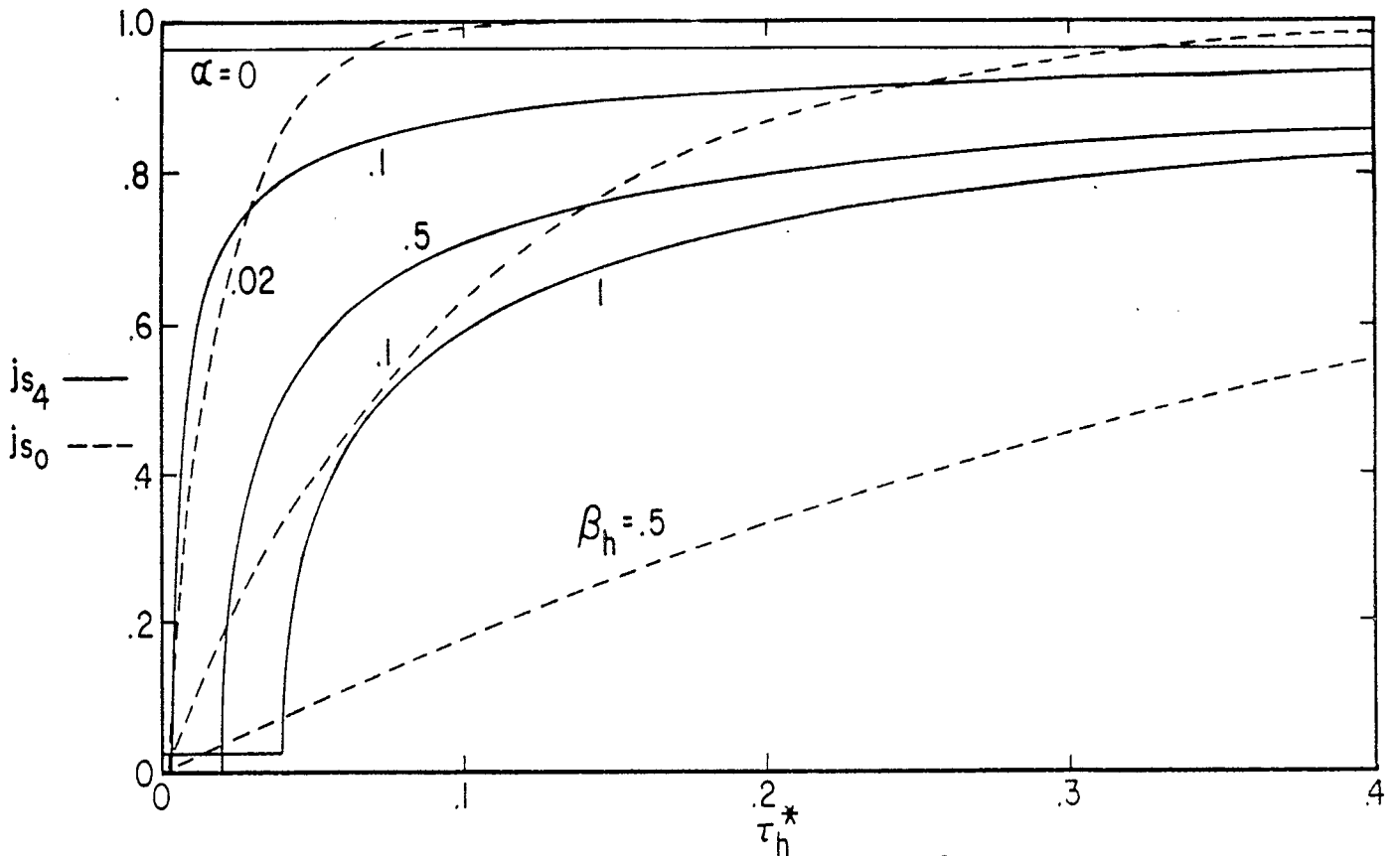


A. j_{s4} FOR VARIOUS α PLUS j_{s0} FOR VARIOUS β_h FOR COMPARISON

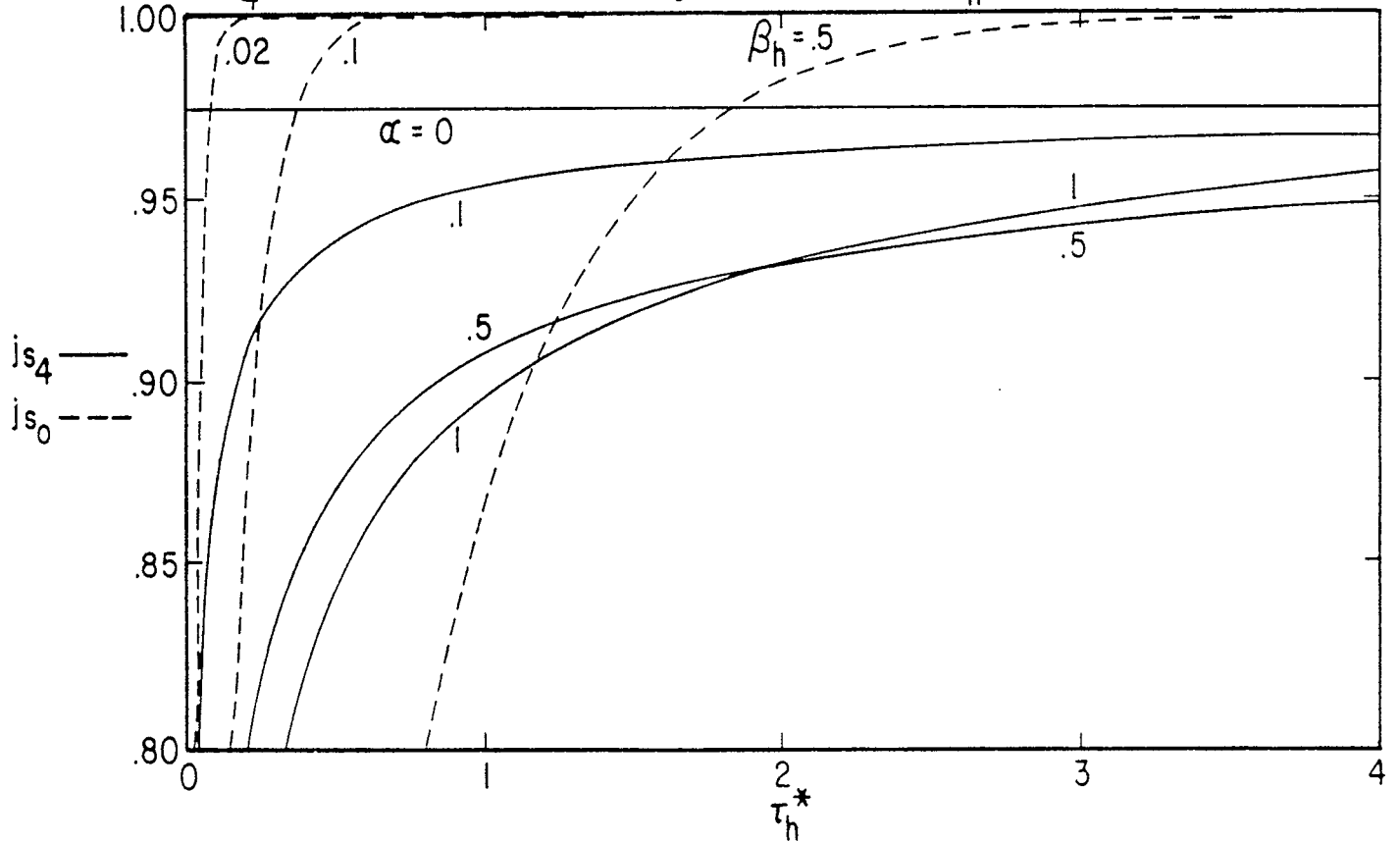


B. SCALES OF A CHANGED TO SHOW LATE-TIME BEHAVIOR

FIGURE 6. SURFACE CURRENT DENSITY INCLUDING BOTH ENDS OF THE ADMITTANCE SHEET; $2\xi/\pi = .1$

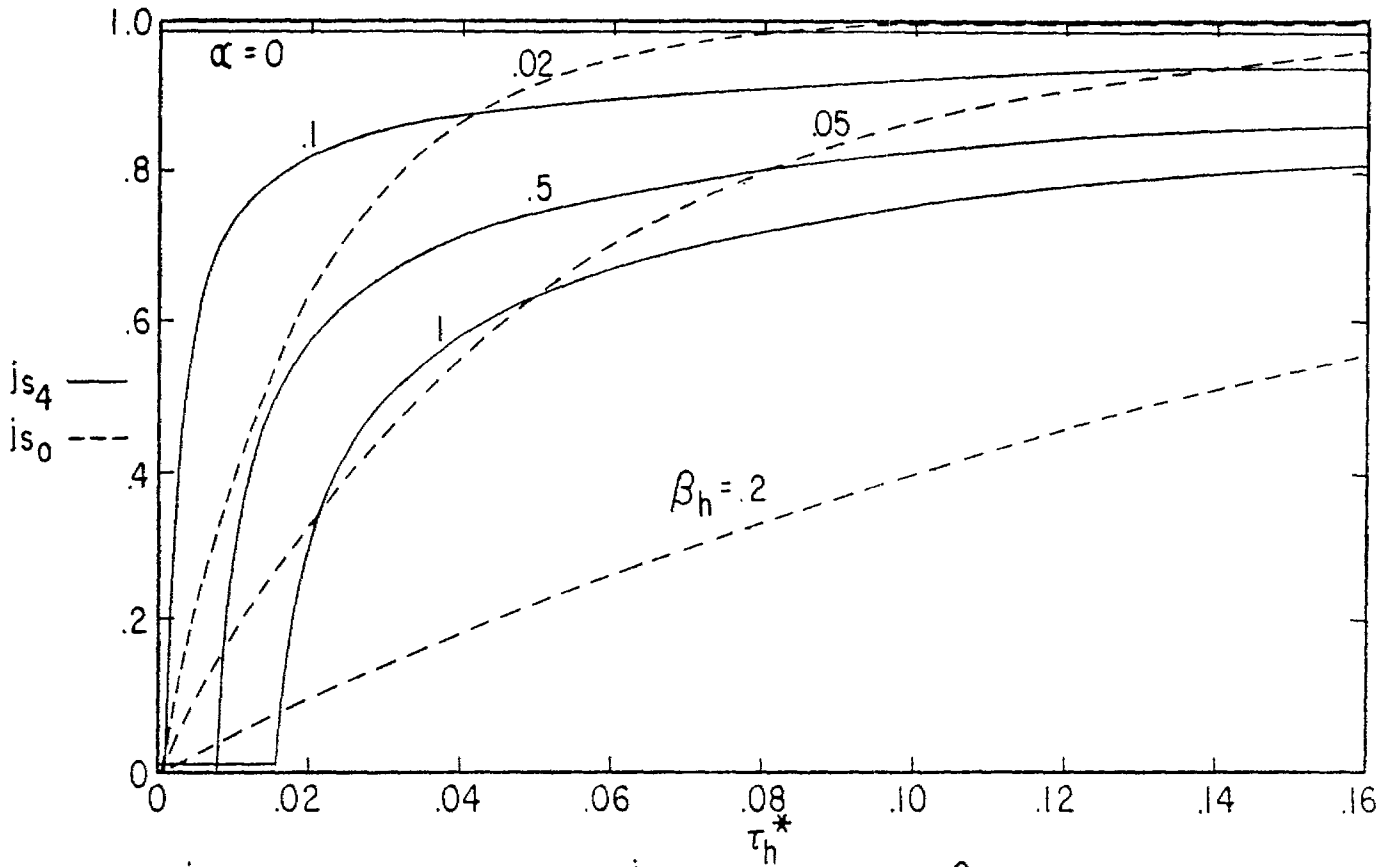


A. j_{s4} FOR VARIOUS α PLUS j_{s0} FOR VARIOUS β_h FOR COMPARISON

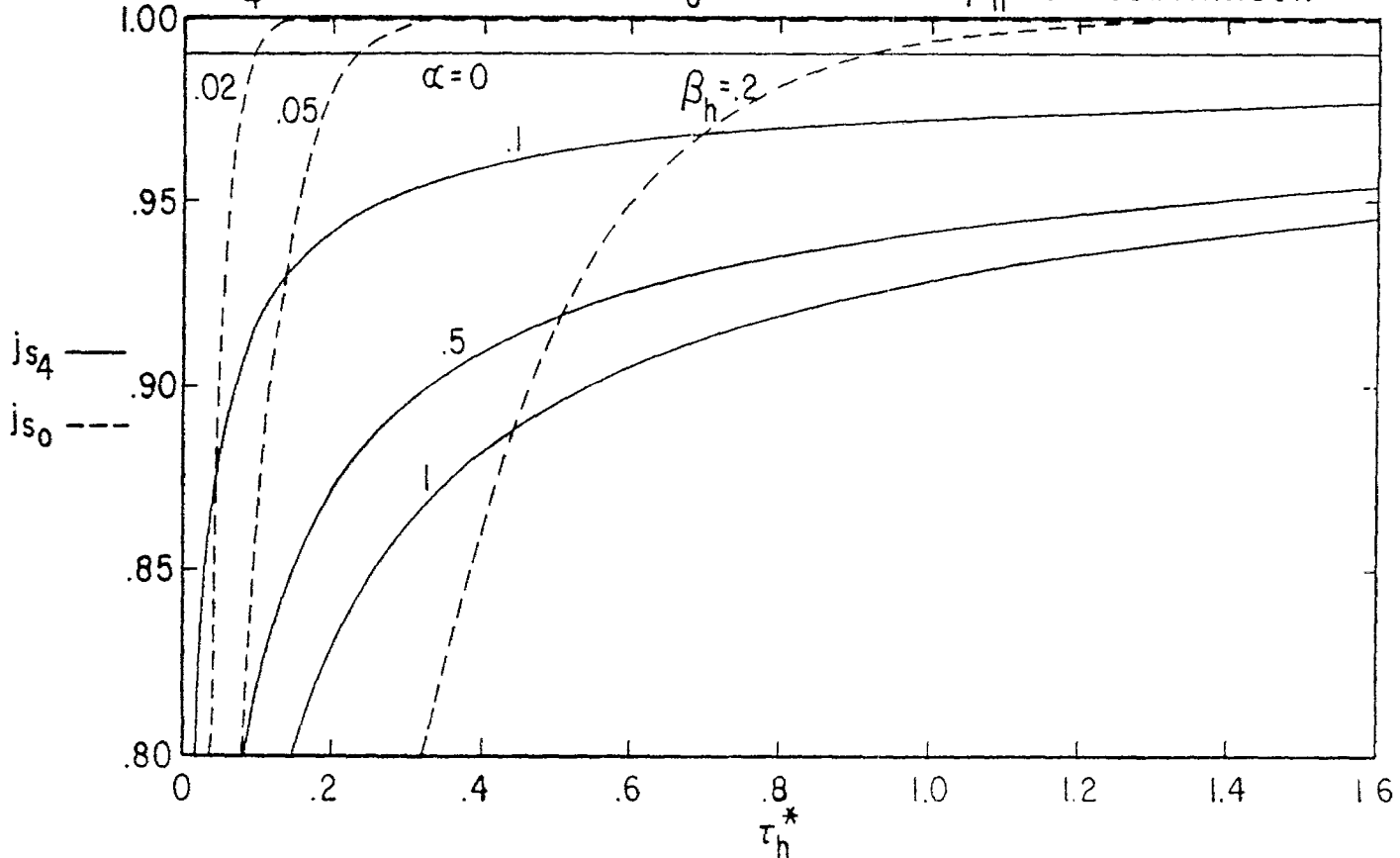


B. SCALES OF A CHANGED TO SHOW LATE-TIME BEHAVIOR

FIGURE 7. SURFACE CURRENT DENSITY INCLUDING BOTH ENDS OF THE ADMITTANCE SHEET: $2\xi/\pi = .05$

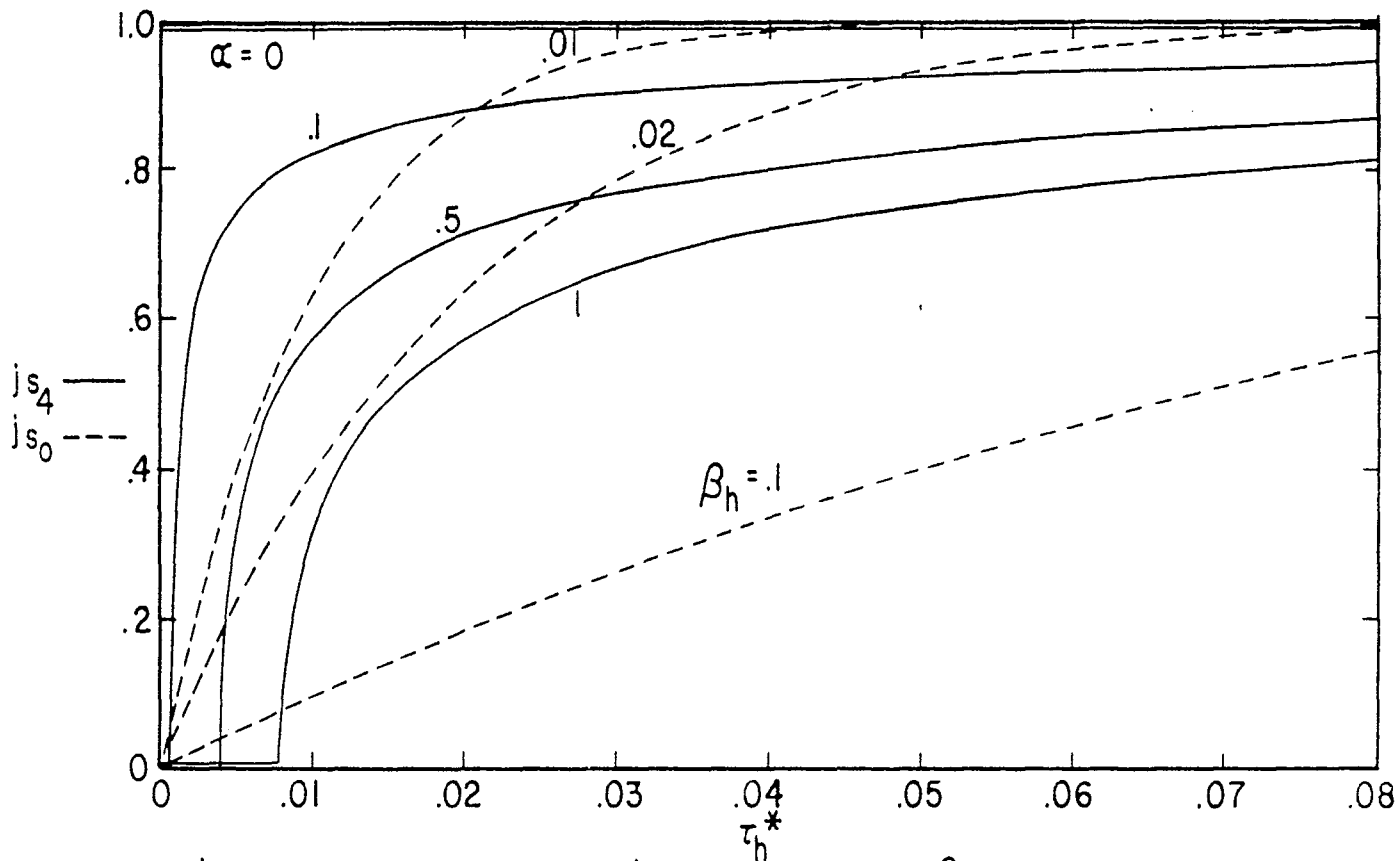


A. j_{s4} FOR VARIOUS α PLUS j_{s0} FOR VARIOUS β_h FOR COMPARISON

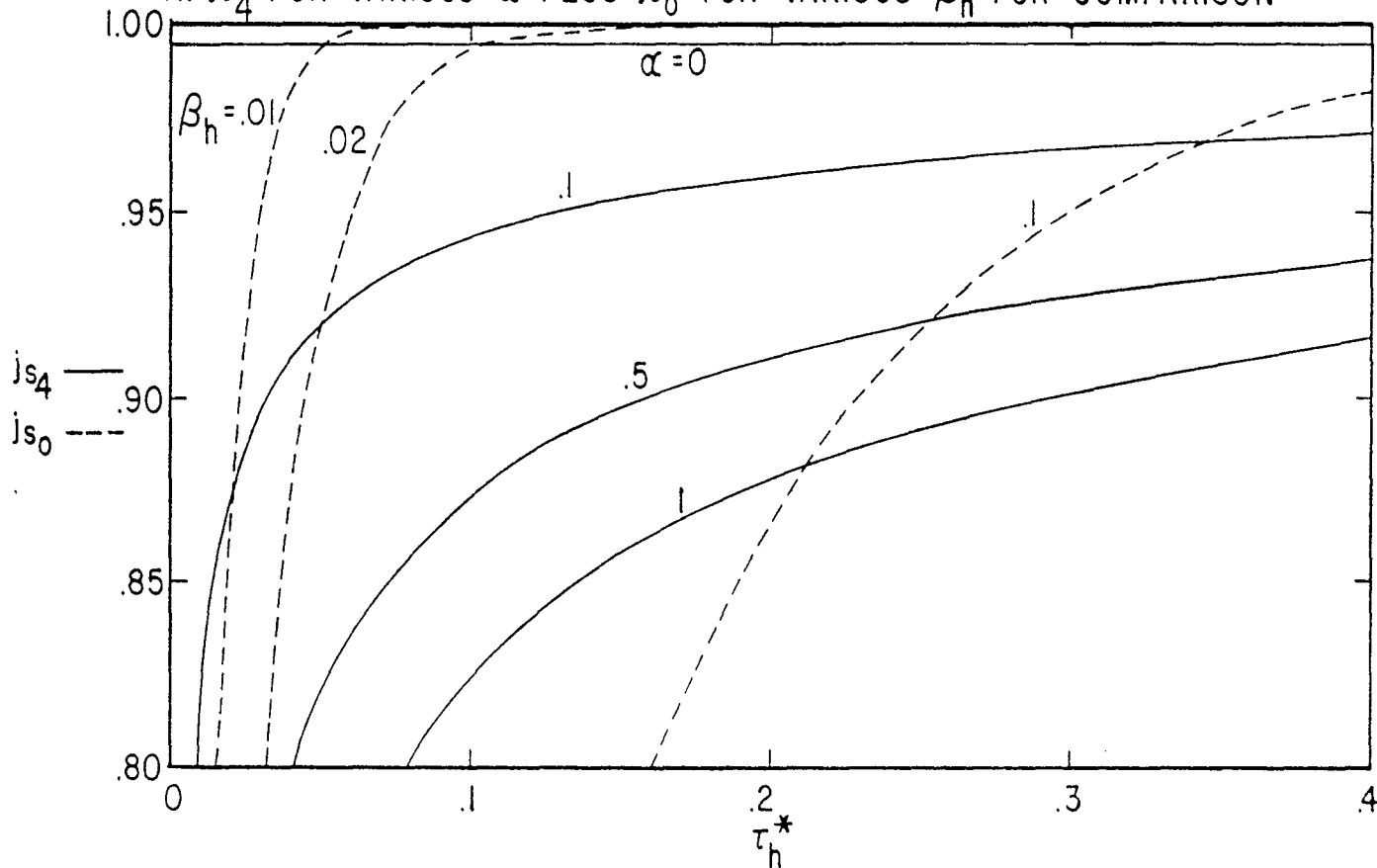


B. SCALES OF A CHANGED TO SHOW LATE-TIME BEHAVIOR

FIGURE 8. SURFACE CURRENT DENSITY INCLUDING BOTH ENDS OF THE ADMITTANCE SHEET: $2\xi / \pi = .02$



A. j_{s4} FOR VARIOUS α PLUS j_{s0} FOR VARIOUS β_h FOR COMPARISON



B. SCALES OF A CHANGED TO SHOW LATE-TIME BEHAVIOR

FIGURE 9. SURFACE CURRENT DENSITY INCLUDING BOTH ENDS OF THE ADMITTANCE SHEET: $2\xi/\pi = .01$